Clinical Cancer Bulletin

ORIGINAL RESEARCH

Open Access

High expression of PAFAH1B3 results in poor prognosis in lung adenocarcinoma patients and is associated with tumor cell pyroptosis genes

Bowen Hu[1†], Lingyu Du[2†], Guangda Yuan[1], Yong Yang[1], Ming Li[3*] and Jie Tan[2*]

Abstract

Background Lung adenocarcinoma (LUAD) is a common cancer with a poor prognosis. Platelet-activating factor acetylhydrolase, isoform Ib, gamma subunit 29 kDa (*PAFAH1B3*) plays an important role in the development of many types of human malignancies. However, the precise role and mechanisms of *PAFAH1B3* in LUAD are still unknown. Therefore, we will initially explore the effect of *PAFAH1B3* on LUAD in this study.

Methods In this study, we first performed a pan-cancer analysis of *PAFAH1B3* expression and prognosis using The Cancer Genome Atlas (TCGA), genotype-tissue expression (GTEx) data, and GEPIA database. Next, the relationship between *PAFAH1B3* expression and LUAD immune infiltration and pyroptosis-related genes was explored by GEPIA database and TIMER database. The effect of *PAFAH1B3* on LUAD was further explored by CCK-8, wound healing, and Transwell assays. Finally, non-coding RNA (ncRNA) that may be involved in the regulation of *PAFAH1B3* was explored using Starbase database analysis.

Results The results found that PAFAH1B3 may be an oncogene in LUAD and has a significant adverse relationship with tumor immune cell infiltration, immune cell biomarkers and pyroptosis-related gene expression. Meanwhile, cell experiments also found that *PAFAH1B3* knockout significantly reduced the proliferation, migration and invasion of A549 cells.

Conclusions *PAFAH1B3* high expression in LUAD patients is associated with poor prognosis, tumor immune infiltration, and cell pyroptosis gene expression.

Keywords *PAFAH1B3*, *DUXAP8*, *Hsa-miR-29c-3p*, Lung adenocarcinoma, Noncoding RNA

†Bowen Hu and Lingyu Du contributed equally to these works.

*Correspondence:
Ming Li
li_m14@fudan.edu.cn
Jie Tan
tj5140992624@163.com
Full list of author information is available at the end of the article

Introduction

Lung cancer has the highest mortality rate of all cancers, and approximately 2.09 million deaths from lung cancer are reported annually worldwide [1]. The 5-year survival rate for lung cancer is only 16%. Lung adenocarcinoma (LUAD) is the most common lung cancer subtype, accounting for 50% of all lung cancer pathological types, and the number one cause of cancer-related death worldwide [2]. Despite the ongoing development of medical technology and progress in diagnostic imaging, minimally invasive thoracoscopic surgery and postoperative adjuvant therapy, the incidence of LUAD is increasing each year and patient prognosis remains unsatisfactory. Therefore, better understanding of the molecular mechanisms of LUAD is critical to identify new effective therapy modalities and prognostic biomarkers.

Platelet-activating factor acetylhydrolases (PAF-AHs) are a class of diverse isozymes involved in a variety of physiological and pathological processes including prognosis, angiogenesis, inflammatory responses, wound healing, and tumor growth. Previous studies have found that high expression of *PAFAH1B3* gene affects the proliferation and migration of gastric cancer cells and is an oncogene of gastric cancer [3]. The results show that *PAFAH1B3* promotes the proliferation, migration and invasion capacity of papillary thyroid carcinoma cells(PTC), and the increase of *PAFAH1B3* expression is likely to trigger tumor cell lymph node metastasis in PTC patients [4].

Increasing evidence has shown that *PAFAH1B3* plays an important role in the development and progression of several human malignancies, including LUAD [5]. However, knowledge of *PAFAH1B3* in LUAD is limited, and more research is required.

Some ncRNAs (including miRNAs, lncRNAs and circRNAs) interact through the ceRNA mechanism and participate in the regulation of gene expression [6]. miRNAs bind to the 3′ and 5′ UTRs of target mRNAs and inhibit target gene expression. lncRNAs can increase mRNA expression by competitively binding to shared miRNAs [7]. We speculate that *PAFAH1B3* may also be regulated by this mechanism, and therefore we will initially explore its regulatory mechanism.

Methods

Analysis of TCGA data

mRNA expression data from 33 cancer types was retrieved from TCGA database (https://portal.gdc.cancer.gov/) (Fig. 1A). Data were then normalized and evaluated for differential expression of *PAFAH1B3* using the R program limma. TCGA database was also used to examine the expression levels of *hsa-miR-29c-3p* and *hsa-miR-101-3p* in LUAD and normal controls. TCGA database was also used for survival analysis of LUAD in accordance with *hsa-miR-29c-3p* expression.

Analysis of the GEPIA database

GEPIA is a web-based tool for profiling and analyzing interactions between genes in both cancer and normal samples [8]. The expression of *PAFAH1B3* and lncRNAs in several types of human malignancies was examined using GEPIA. Survival analysis of *PAFAH1B3*, including overall survival (OS) and disease-free survival (DFS), was performed in 12 different cancer types using GEPIA. The predictive ability of potential lncRNAs in LUAD was evaluated using GEPIA. The GEPIA database was also used to evaluate the connection between *PAFAH1B3* and immune cell biomarkers. The selection criteria $|R|>0.1$ and *P*-value less than 0.05 were used to determine statistical significance.

Prediction of miRNAs

Seven target gene prediction algorithms, including PITA, RNA22, miRmap, DIANA-microT, miRanda, PicTar, and TargetScan, were used to predict the upstream binding miRNAs of *PAFAH1B3*. We focused on miRNAs that were identified in two or more of the target gene prediction tools mentioned above. The collected miRNAs were considered as candidate miRNAs that regulate *PAFAH1B3*.

Analysis of Starbase database

Starbase (http://starbase.sysu.edu.cn/) is a database used for studying miRNAs [9]. This database was used for miRNA-*PAFAH1B3*, lncRNA-*hsa-miR-29c-3p*, lncRNA-*hsa-miR-101-3p*, and lncRNA-*PAFAH1B3* expression correlation analysis in LUAD. Starbase was used to predict candidate lncRNAs that may bind to let-7c-5p.

TIMER database analysis

TIMER (https://cistrome.shinyapps.io/timer/) is a database used for the analysis of tumor infiltrating immune cells [10]. TIMER was used to analyze the correlation between *PAFAH1B3* expression levels and the level of immune cell infiltration in LUAD. The correlation of *PAFAH1B3* expression with pyroptosis genes in LUAD was also assessed using the TIMER database.

Immunohistochemistry

We collected 60 cases of postsurgical lung adenocarcinoma tissue and normal lung tissue (25 men, 35 women, aged between 45 and 60 years) from the Department of Thoracic Surgery, Suzhou Hospital, Nanjing Medical University.Tissue sections were first treated in 3% H_2O_2 for 15 min at room temperature. After blocking with goat serum for 1 h, the slides were treated with primary

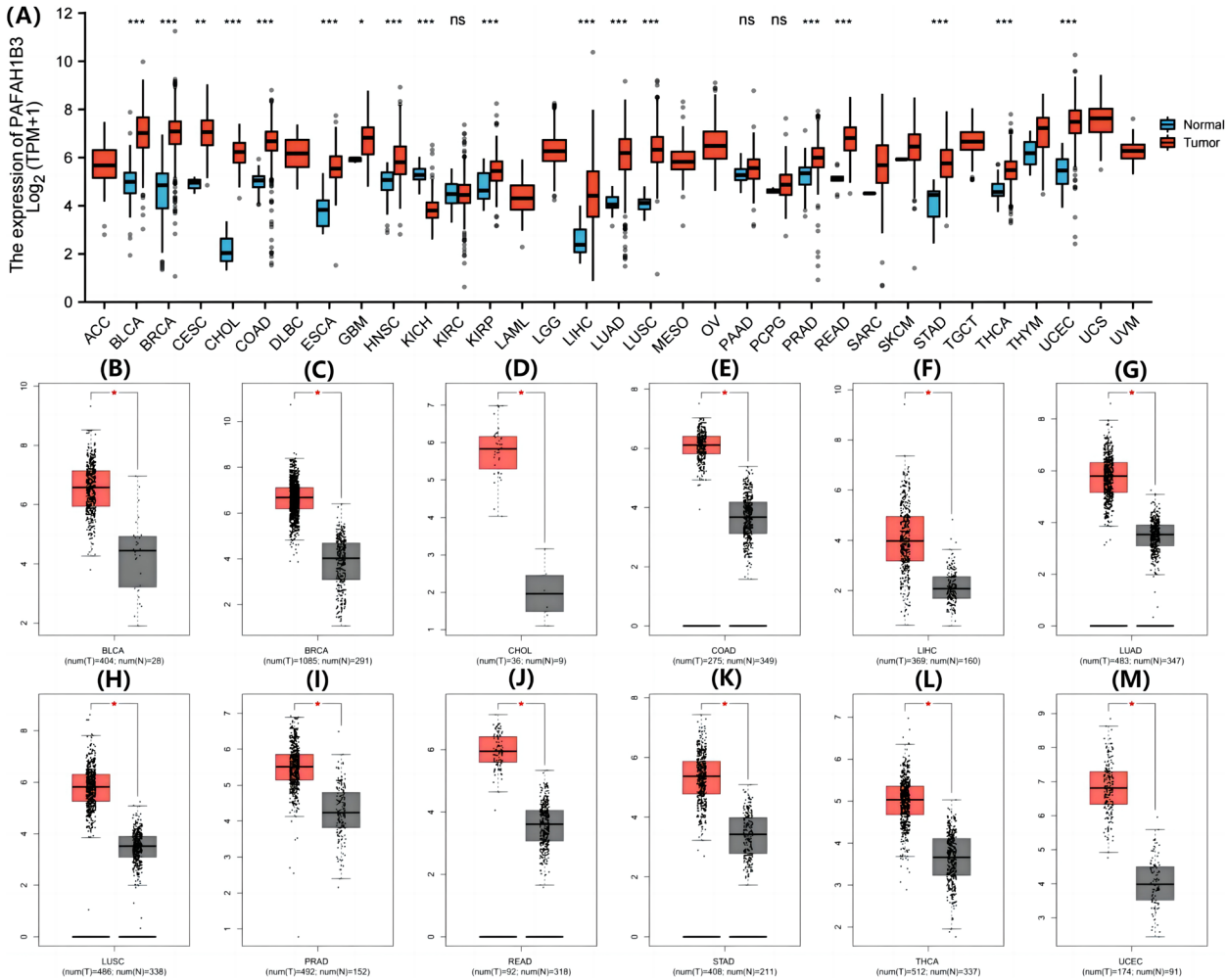

Fig. 1 Analysis of *PAFAH1B3* expression in cancer. **A** The expression of *PAFAH1B3* in 33 types of human cancer in TCGA data. **B**–**M** *PAFAH1B3* expression in GEPIA database. ∗$P < 0.05$; ∗∗$P < 0.01$; ∗∗∗$P < 0.001$

antibodies against *PAFAH1B3* (1:100, Abcam,Cambridge, England, ab241288). The sections were rinsed three times in PBS and incubated with goat-anti-rabbit IgG secondary antibodies (China Fuzhou Maixin Biotech). The slices were washed three times in PBS for 5 min each and then treated with streptavidin-conjugated HRP (China Fuzhou Maixin Biotech). Images were captured with an Olympus camera and corresponding software(Leica: BOND MAX, Switzerland). Two independent pathologists graded the staining results. The staining intensity of the sections was quantified by the IHC tool in Image J software (National Institutes of Health, America). Staining intensity was quantified as 0 (no staining), 1 + (weak staining), 2 + (moderate staining) or 3 + (strong staining) and frequency was quantified as the percentage of relevant cells (e.g., viable tumor cells) exhibiting staining at the appropriate subcellular location. H-scores were then calculated based on the percentage of stained cells at each intensity level: H-score = cell staining intensity score × percentage of staining.

Quantitative real-time PCR

Total RNA was isolated using TRIzol from A549,H460, H1299,H292,BEAS-2B cells (ATCC,America). Reverse transcription was performed using a PCR amplifier (ABI, USA) to generate cDNA. For quantitative PCR experiments, the following reaction conditions were used: pre-denaturation at 95 ℃ for 10 min, and 40 cycles of denaturation at 95 ℃ for 10 s, annealing at 60 ℃ for 20 s, and extension at 72 ℃ for 34 s. The Ct value (threshold cycle) was determined by manually setting the threshold at the lowest point of each logarithmic amplification curve's parallel climb. β-actin mRNA was used as the internal reference. Data were analyzed using the $2^{-\Delta\Delta Ct}$

method. PCR primers were synthesized by Shanghai Bioengineering Technology Service Co., Ltd. and the primer sequences were as follows: *PAFAH1B3*: F: 5′-CGGATC AAGAGATTCCAGGTTC-3′, R: 5′-CCGGAGGGAGAG GATTCTT-3′.

Transwell invasion assay

A549 cells were inoculated at 5×10^3 cells/cm^2 in cell culture dishes and the medium was changed every 2–3 days until cells achieved 70%–90% confluence. The cells (1×10^5/mL) were then inoculated in Transwell chambers (coated with 500 μL of Matrigel gel). The cells in the top chambers were incubated in serum-free medium and medium containing 10% FBS was included in the bottom chamber. Plates were incubated for 48 h. The chambers were removed, and cells were fixed in paraformaldehyde at 4 ℃ for 30 min and left to stand at room temperature for 20 min. Next, 750 μL of 0.1% crystalline violet solution was added and cells were incubated at room temperature for 20 min. The cells were washed three times with water and the number of invaded cells was counted under a microscope (Zeiss Germany).

CCK-8 assay

The OD of the standard was first measured at a wavelength of 450 nm using the cells to be measured and a standard curve was plotted. Cells were added to a 96-well plate at 100 μL per (10^5/mL) well and incubated at 37 ℃ with 5% CO_2. Next, 10 μL of CCK-8 solution was added to each well and cells were incubated for 2 h. The OD was recorded by measuring the absorbance at 450 nm using a microplate reader. Cell viability was calculated as follows = ([As-Ab] / [Ac-Ab]) × 100%.

shRNA and cell transfection

The pLKO.1G GFP-shRNA plasmid for *PAFAH1B3* was purchased from Addgene. The *PAFAH1B3*-specific shRNA sequences were: sh-*PAFAH1B3*#1: 5′- CACCGG AAGCGAAGGTTCCTGATTCCTCGAGGAATCAGG AACCTTCGCTTCC-3′; and sh-*PAFAH1B3*#2: 5′- CAC CGCCTTCCCACAACATTAAACTCTCGAGAGTTT AATGTTGTGGGAAGGC-3′. Cells were transfected with shRNA (1 μg, 50 pmol) using Lipofectamine 2000 following the manufacturer's instructions. Cells were incubated for 48 h and then examined by qRT-PCR.

Wound healing assay

Single cell suspensions were inoculated in 6-well culture plates at 0.5 cm intervals. The cells were rinsed three times with PBS to remove the scratched cells and serum-free medium was added. The marker was finally wiped from the back of the 6-well plate and photographed under a 4× microscope. Cells were photographed at 24 and 48 h. After subsequently opening the images using Image J software, six horizontal lines were randomly scratched and the mean average of the intercellular distances was calculated. Cell migration rate (wound healing rate) = (mean value of initial intercellular distance—mean value of intercellular distance at time t)/mean value of initial intercellular distance.

Statistical analysis

The statistical analyses in this study were generated automatically *via* the online database stated above. *P*-values less than 0.05 or log-rank *P*-values less than 0.05 were considered statistically significant.

Results

Pan-cancer analysis of PAFAH1B3 expression

To evaluate the potential function of *PAFAH1B3* in carcinogenesis, we first examined its expression in 33 human cancers using UCSC XENAdata in TCGA database. *PAFAH1B3* was significantly elevated in 18 cancer types, including glioblastoma multiforme (GBM), uterine corpus endometrial carcinoma (UCEC), lung adenocarcinoma (LUAD), bladder uroepithelial carcinoma (BLCA), breast invasive carcinoma (BRCA), cervical and endocervical carcinoma (CESC), cholangiocarcinoma (CHOL), colon adenocarcinoma (COAD), esophageal carcinoma (ESCA), squamous cell carcinoma of the head and neck (HNSC), liver hepatocellular carcinoma (LIHC), ovarian serous cystadenocarcinoma (OV), lung squamous cell carcinoma (LUSC), stomach adenocarcinoma (STAD), thyroid carcinoma (THCA) and kidney renal clear cell carcinoma (KIRC), kidney renal papillary cell carcinoma (KIRP), liver hepatocellular carcinoma (LIHC), prostate adenocarcinoma (PRAD), rectal adenocarcinoma (READ), compared with paracancerous tissue. We then examined *PAFAH1B3* expression in these 18 cancer types using the GEPIA database. *PAFAH1B3* expression was significantly higher in the following cancer types compared with corresponding non-cancerous tissue samples: BLCA, BRCA, CHOL, COAD, LIHC, LUAD, LUSC, PRAD, READ, STAD, THCA, and UCEC (Fig. 1B–M).

The prognostic values of PAFAH1B3 in human cancer

We next performed survival analysis in accordance with *PAFAH1B3* expression in BLCA, BRCA, CHOL, COAD, LIHC, LUAD, LUSC, PRAD, READ, STAD, THCA, and UCEC using the GEPIA database. High expression of *PAFAH1B3* in LIHC and LUAD was prognostically unfavorable in terms of OS (Fig. 2). Increased expression of *PAFAH1B3* in all cancer types also indicated a poor prognosis for LIHC and LUAD in terms of DFS (Fig. 3). *PAFAH1B3* did not indicate prognosis in other cancer

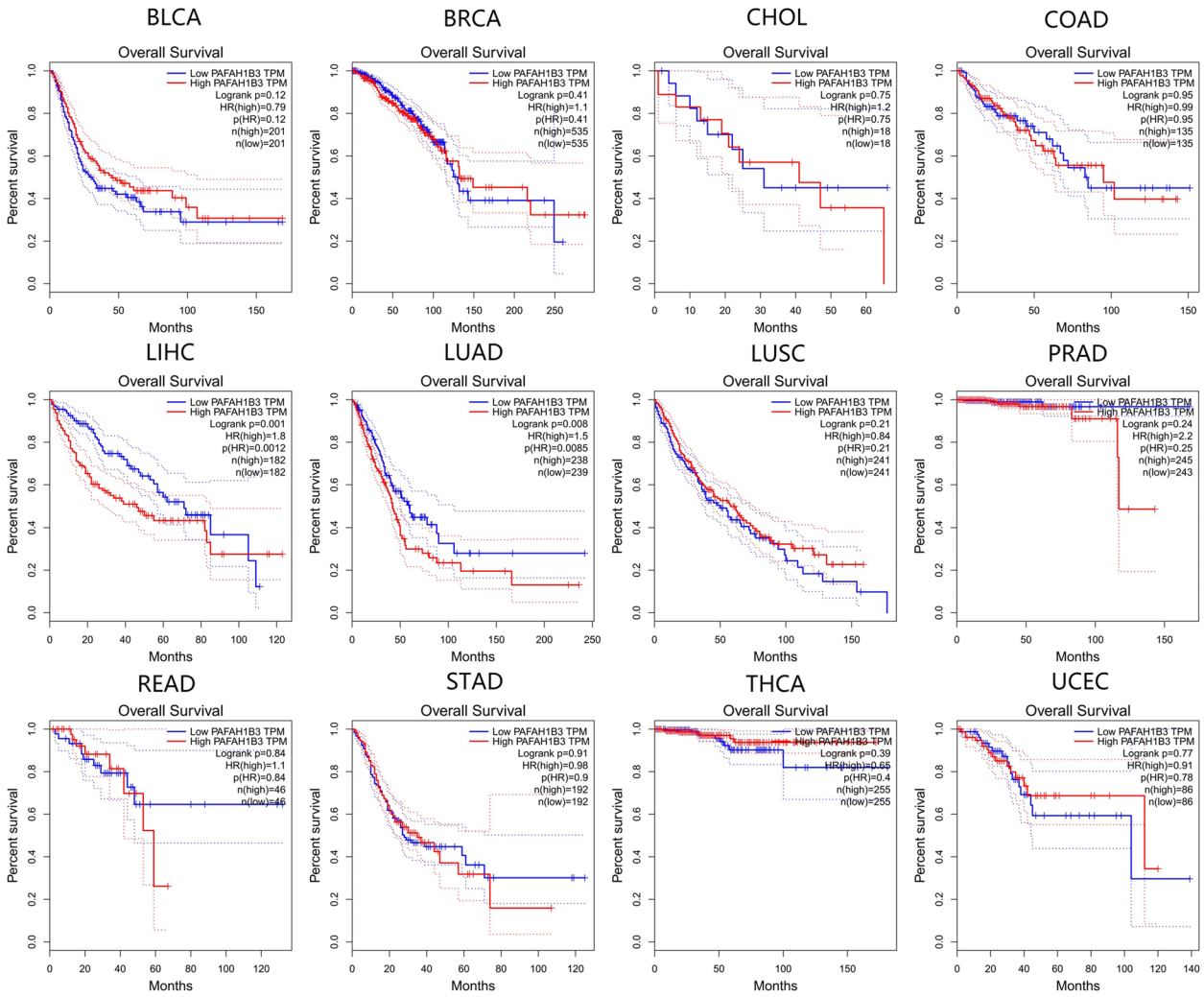

Fig. 2 Overall survival (OS) of cancer patients in accordance with *PAFAH1B3* expression in GEPIA database

types. These findings indicated that *PAFAH1B3* may be a biomarker for poor prognosis in patients with LUAD.

PAFAH1B3 is highly expressed in LUAD and correlates with the malignancy of the tumor

Our results above showed that *PAFAH1B3* was significantly highly expressed in lung adenocarcinoma and closely associated with the prognosis of lung adenocarcinoma patients. We next performed immunohistochemistry of *PAFAH1B3* in tumor tissues and normal lung tissues from 60 lung adenocarcinoma patients and found that *PAFAH1B3* was significantly highly expressed in the lung adenocarcinoma tissues compared with normal lung tissues (Fig. 4A, B), which was consistent with our previous findings.

We next explored the role of *PAFAH1B3* in lung adenocarcinoma through in vitro experiments. qRT-PCR experiments suggested that *PAFAH1B3* was expressed at the highest level in the A549 cell line compared with human lung normal epithelial cells BEAS-2B (Fig. 4C). We constructed an A549 cell line with knockdown of *PAFAH1B3* and verified the successful knockdown by qRT-PCR (Fig. 4D). CCK-8, wound healing and Transwell assays showed that the proliferation, migration and invasive abilities of A549 cells were significantly inhibited after *PAFAH1B3* knockdown (Fig. 4E–G).

Prediction and search for upstream miRNAs of PAFAH1B3

Studies have shown that ncRNAs play a key role in controlling gene expression. To evaluate whether *PAFAH1B3* is regulated by miRNAs, we used the starBase database to predict the potential miRNAs that may bind to *PAFAH1B3*, and the results identified 14 miRNAs. We used Cytoscape software to create a miRNA-*PAFAH1B3* regulatory network (Fig. 5A). miRNAs bind the 3′ and 5′ UTRs of target mRNAs to suppress the

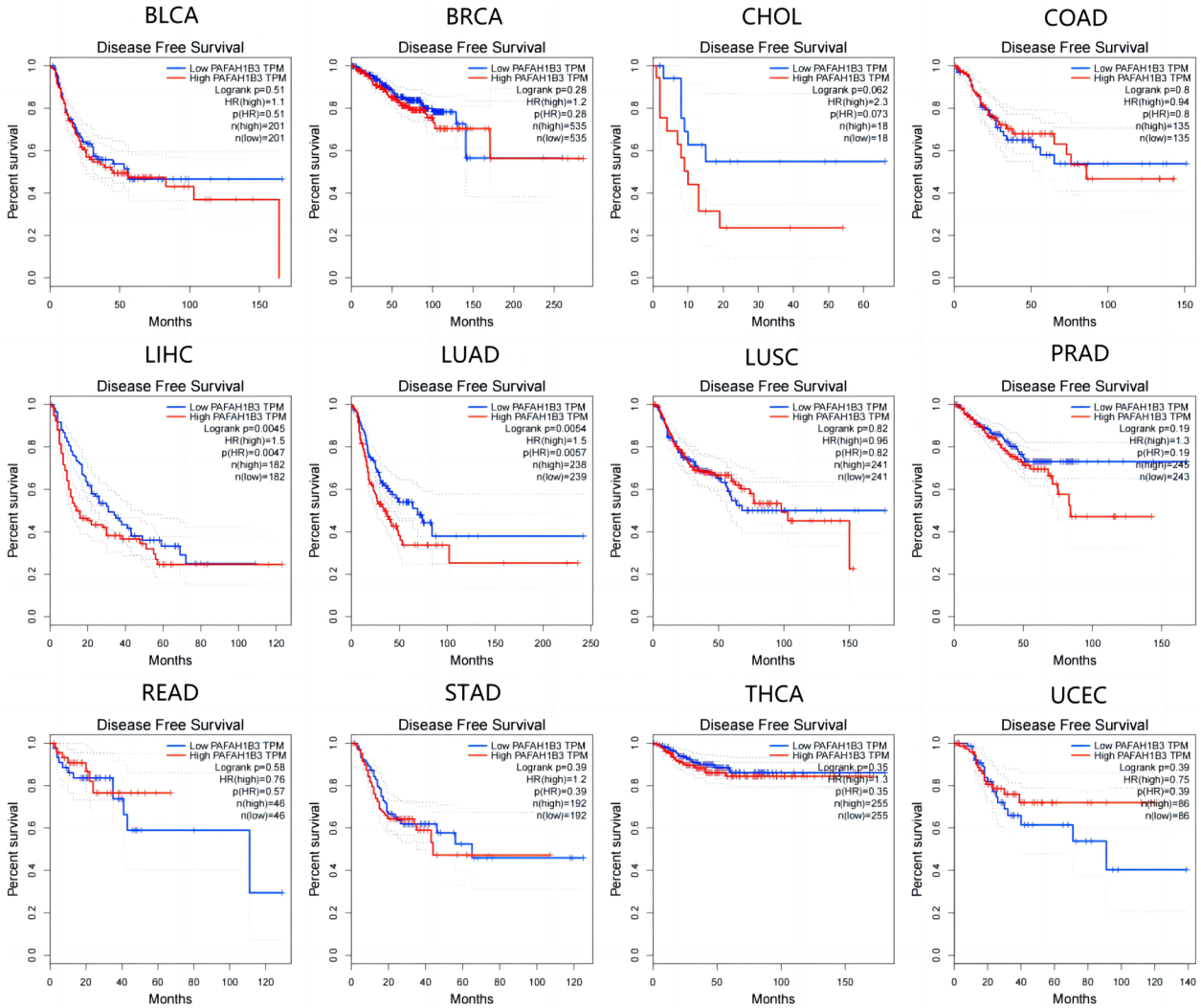

Fig. 3 Disease-free survival (DFS) of cancer patients in accordance with *PAFAH1B3* expression in GEPIA database

expression of the target gene. We performed expression correlation analysis and found that *PAFAH1B3* was significantly negatively linked with *hsa-miR-29c-3p* and *hsa-miR-101-3p* and positively correlated with *hsa-miR-301a-3p* and *hsa-miR-3619-5p* in LUAD (Fig. 4B). We then investigated the expression and prognostic value of *hsa-miR-29c-3p* and *hsa-miR-101-3p* in LUAD using TCGA LUAD (lung adenocarcinoma) miRNAseq database. The results showed that *hsa-mi-R-29c-3p* was significantly downregulated in LUAD and its upregulation was positively correlated with patient prognosis (Fig. 5C, D). *hsa-miR-101-3p* was significantly down-regulated in LUAD but its up-regulation was not correlated with patient prognosis (Fig. 5E, F). These findings suggest that *hsa-miR-29c-3p* may play a role in regulating *PAFAH1B3* in LUAD.

Prediction and analysis of lncRNAs upstream of hsa-miR-29c-3

The Starbase database was then used to examine potential upstream lncRNAs of *hsa-miR-29c-3p* and 30 potential lncRNAs were identified. The Cytoscape program was used to build the *hsa-miR-29c-3p* regulatory network (Fig. 6A). The expressions of these lncRNAs in LUAD were then assessed using GEPIA. Only double homeobox A pseudogene 8 *(DUXAP8)* was highly elevated in LUAD compared to normal controls (Fig. 6B). The prognostic significance of *DUXAP8* in LUAD was evaluated. LUAD patients with increased *DUXAP8* expression had a shorter life expectancy (Fig. 6C). Some lncRNAs function as competitive endogenous RNAs (ceRNAs) by competitively binding to miRNAs resulting in increased mRNA expression. The expression association between *DUXAP8*

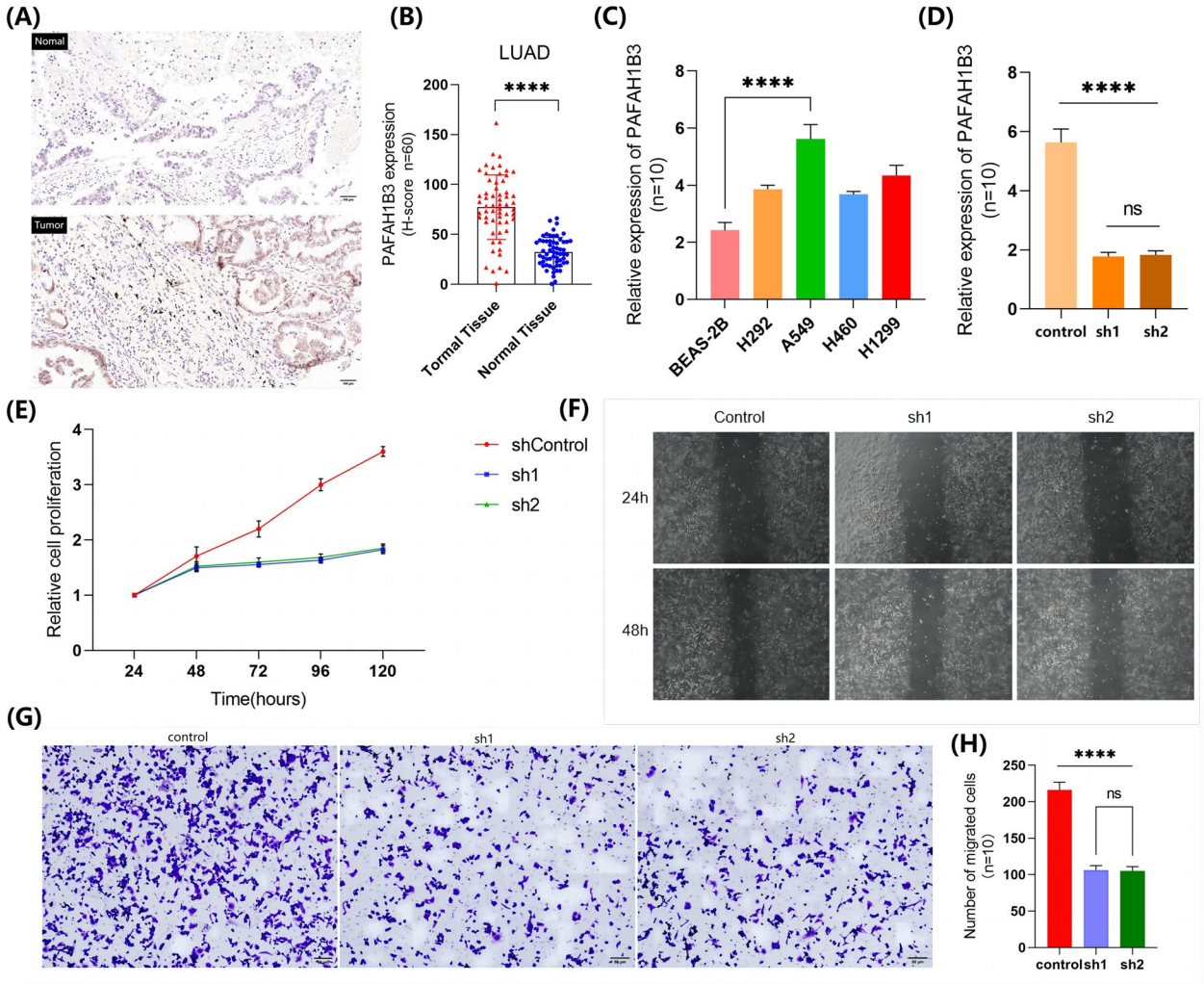

Fig. 4 *PAFAH1B3* was highly expressed in lung adenocarcinoma and its downregulation reduced malignant activities of lung adenocarcinoma cells. **A** Immunohistochemistry of *PAFAH1B3* in lung adenocarcinoma and normal lung tissues; **B** *PAFAH1B3* expression was significantly lower in tumor tissues compared with normal tissues; **C** qRT-PCR assay showed that *PAFAH1B3* expression was higher in human lung cancer cell lines than in human lung normal epithelial cells; **D** The expression of *PAFAH1B3* in A549 cells was greatly reduced after lentivirus-mediated knockdown of *PAFAH1B3*; **E** CCK-8 assay revealed that A549 cell growth was inhibited following *PAFAH1B3* knockdown; **F** Scratch assay showed that the migration ability of A549 cells was significantly reduced after knockdown of *PAFAH1B3*; **G**–**H** Transwell assay showed that the invasive ability of A549 cells was significantly reduced after knockdown of *PAFAH1B3*

and *hsa-miR-29c-3p* or *PAFAH1B3* in LUAD was further investigated using the Starbase database (Table 1). From the results of expression, survival, and correlation analyses, *DUXAP8* may be a promising upstream lncRNA of the *hsa-miR-29c-3p*/*PAFAH1B3* axis in LUAD.

The expression of *DUXAP8* was negatively correlated with *hsa-miR-29c-3p* and positively with *PAFAH1B3* expression. This fits with the mechanism by which ncRNAs participates in the regulation of gene expression through a ceRNA manner.

PAFAH1B3 corresponds with immune cell infiltration in LUAD

PAFAH1B3 also serve an important role in the immune system. We observed substantial alterations in the levels of B cells, $CD4^+$ T cells, macrophages, neutrophils, and dendritic cell infiltration in LUAD with different copy numbers of *PAFAH1B3* (Fig. 7A). Correlation analysis may potentially provide more pertinent insights regarding the function and mechanism of *PAFAH1B3*. We thus examined the relationship between *PAFAH1B3*

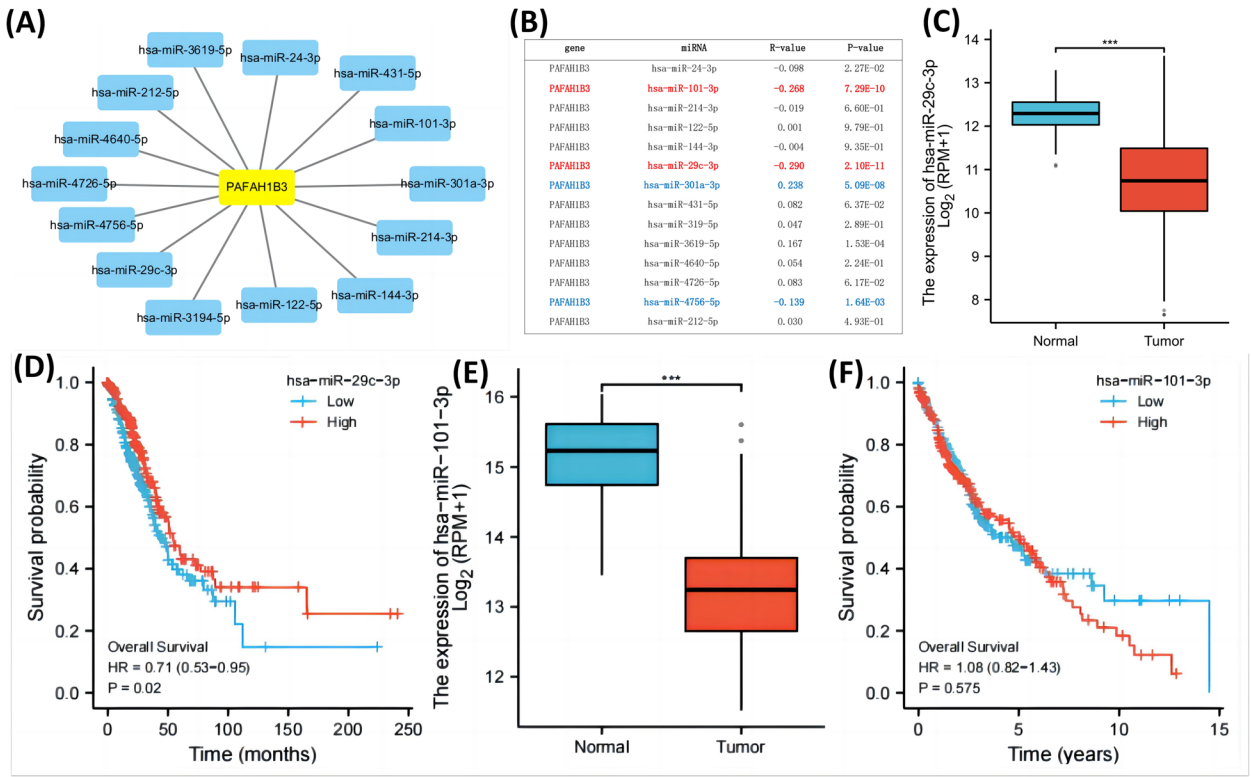

Fig. 5 *hsa-miR-29c-3p* is a potential upstream miRNA of *PAFAH1B3* in LUAD. **A** A regulatory network of miRNA and *PAFAH1B3* was created using Cytoscape software. **B** Starbase database analysis of the association between predicted miRNAs and *PAFAH1B3* in LUAD. **C**, **D** The expression and prognostic significance of *hsa-miR-29c-3p* in LUAD and normal control samples was examined in TCGA database. **E**, **F** The expression and prognostic significance of *hsa-miR-101-3p* in LUAD and normal control samples was examined in TCGA database

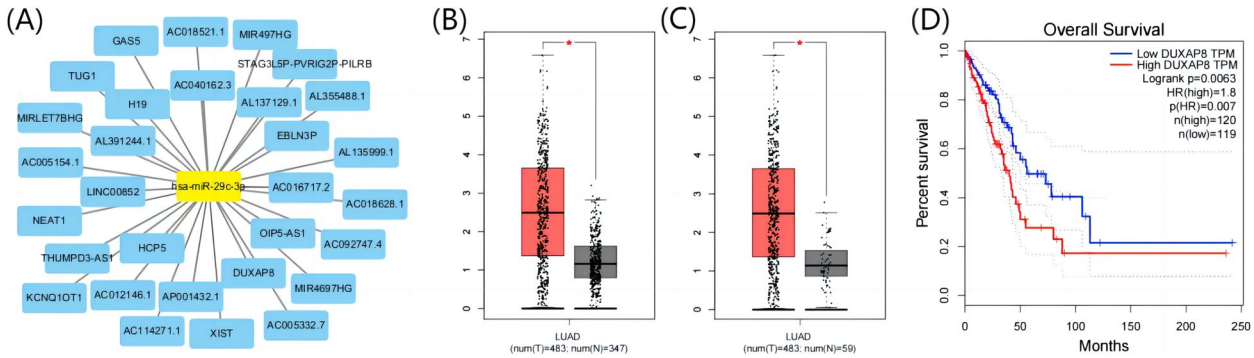

Fig. 6 Expression analysis and survival analysis of lncRNAs upstream of *hsa-miR-29c-3p* in LUAD. **A** The lncRNA regulatory network of *hsa-miR-29c-3p*. **B, C** Expression of *hsa-miR-29c-3p* in TCGA LUAD compared with "TCGA normal" or "TCGA and GTEx normal" data. **D** OS analysis of LUAD in accordance with *DUXAP8* expression. **P*< 0.05

expression and immune cell infiltration. As shown in Fig. 7B–G, *PAFAH1B3* expression showed a significant negative correlation with all immune cells analyzed, including B cells, $CD8^+$ T cells, macrophages, neutrophils and dendritic cells in LUAD.

Correlation of PAFAH1B3 expression with biomarkers of immune cells in LUAD

To further investigate the role of *PAFAH1B3* in immune cell infiltration in LUAD, we determined the correlation of *PAFAH1B3* expression with immune cell biomarkers in LUAD using the GEPIA database. We

Table 1 Correlation analysis between lncRNA and *hsa-miR-29c-3p* or lncRNA and *PAFAH1B3* in LUAD determined by Starbase database

lncRNA	mRNA	*R* value	*P* value
DUXAP8	Hsa-miR-29c-3p	-0.199	5.56×10^{-6}***
lncRNA	mRNA	*R* value	*P* value
DUXAP8	PAFAH1B3	0.126	3.37×10^{-3}**

** *P* value < 0.01

*** *P* value < 0.001

observed a correlation between *PAFAH1B3* and biomarkers of B cells (*CD19* and *CD79A*), biomarkers of $CD8^+$ T cells (*CD8A* and *CD8B*), biomarkers of $CD4^+$ T cells (*CD4)*, biomarkers of M1 macrophages (*NOS2, IRF5* and *PTGS2*), biomarkers of M2 macrophages (*CD163, VSIG4* and *MS4A4A*), biomarkers of neutrophils (*ITGAM* and *CCR7)* and biomarkers of dendritic cells (*HLA-DPB1, HLA-DRA, HLA-DPA1, CD1C, NRP1* and *ITGAX*) (Table 2). These findings provide further evidence that *PAFAH1B3* has an important association with immune cell infiltration in LUAD.

PAFAH1B3 was negatively associated with B-cell biomarkers (*CD79A*), $CD8^+$ T-cell biomarkers (*CD8A*), $CD4^+$ T-cell biomarkers (*CD4*), M1 macrophage biomarkers (*IRF5*), biomarkers for M2 macrophages (*CD163, VSIG4* and *MS4A4A*), biomarkers for neutrophils (*ITGAM* and *CCR7*) and biomarkers of dendritic cells (*HLA-DPB1, HLA-DRA, HLA-DPA1, CD1C, NRP1* and *ITGAX*) were negatively correlated.

Relationship between PAFAH1B3 and pyroptosis genes of LUAD

As we mentioned above, platelet-activated factor acetylhydrolases (PAF-AHs) are a variety of isoenzymes involved in a variety of physiological and pathological processes, including the inflammatory response. We

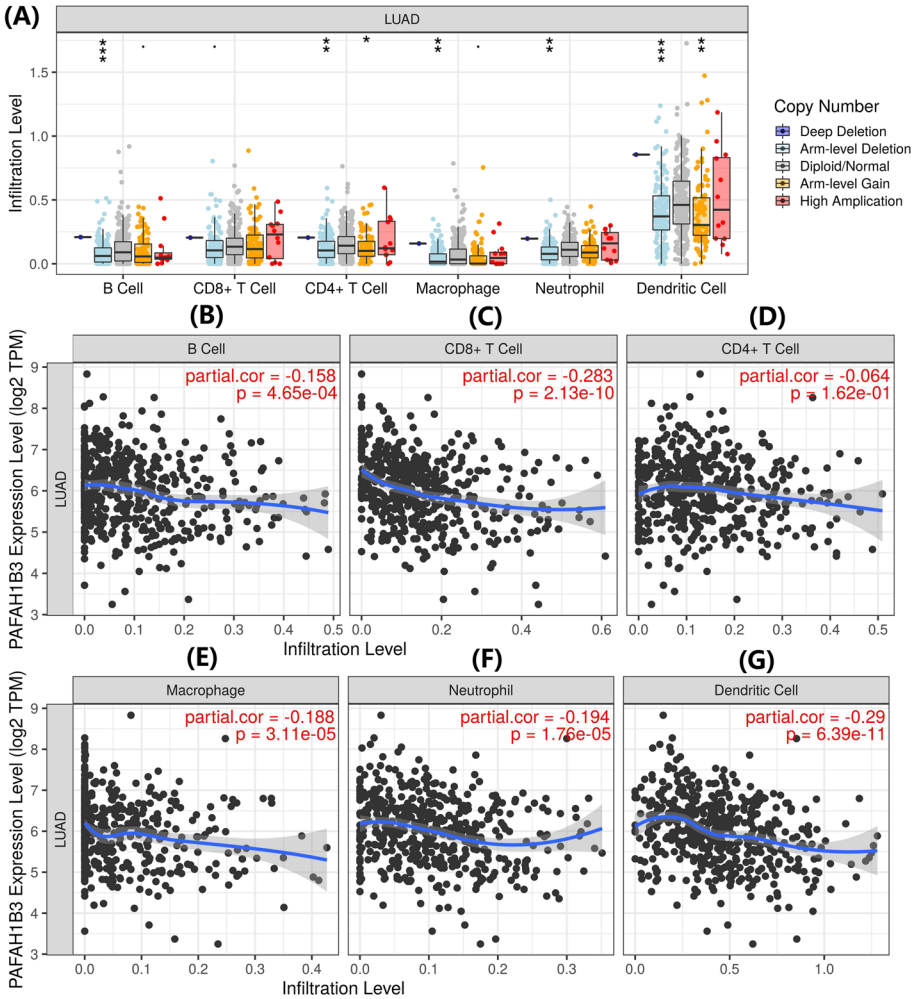

Fig. 7 Relationship between immune cell infiltration and PAFAB1H3 expression in LUAD. **A** Infiltration levels of various immune cells in LUAD with different copy numbers of PAFAB1H3. **B**–**G** Correlation of *PAFAH1B3* expression levels in HCC with infiltration levels of B cells (**B**), $CD8^+$ T cells (**C**), $CD4^+$ T cells (**D**), macrophages (**E**), neutrophils (**F**) and dendritic cells (**G**)

Table 2 Correlation analysis between *PAFAH1B3* and biomarkers of immune cells in LUAD determined by GEPIA database

Immune cell	Biomarker	*R* value	*P* value
B cell	CD19	-0. 11	0.019
	CD79A	-0. 14	2.8E-02**
$CD8^+$ T cell	CD8A	-0. 13	4.6E-02**
	CD8B	0.014	0.75
$CD4^+$ T cell	CD4	-0.26	9.6E-09***
MI macrophage	NOS2	0.068	0. 14
	IRF5	-0. 15	1.2E-03**
	PTGS2	0.082	4.8E-
M2 macrophage	CD163	-0. 17	1.4E-04***
	VSIG4	-0.23	5. 1E-07***
	MS4A4A	-0.23	2.7E-07***
Neutrophil	CEACAM8	-0.1	0.029*
	ITGAM	-0.23	1.8E-07***
	CCR7	-0. 15	9.8E-04***
Dendritic cell	HLA-DPB1	-0.33	3.9E- 14***
	HLA-DQB1	-0. 16	5E-04***
	HLA-DRA	-0.34	1.3E- 14***
	HLA-DPA1	-0.33	1.3E- 13***
	CD1C	-0. 19	3.2E-05***
	NRP1	-0. 12	6.6E-3**
	ITGAX	-0. 17	2.5E-04***

* *P* value < 0.05

***P* value < 0.01

*** *P* value < 0.001

had to consider the possible involvement of *PAFAH1B3* in apoptosis, which required further evaluating the relationship between *PAFAH1B3* and cell apoptosis in lung adenocarcinoma cells. NOD-like receptor thermal protein domain associated protein 3*(NLRP3),* NOD-like receptor thermal protein domain associated protein 2*(NLRP1),* caspase 1*(CASP1)* and Interferon regulatory factor 2(*IRF2)* are important cell scorch proteins responsible for pyroptosis. Cell pyroptosis is closely associated with tumor progression. Considering the high expression of *PAFAH1B3* as a potential oncogenic and poor prognostic factor in LUAD, we evaluated the relationship between *PAFAH1B3* and *NLRP3, NLRP1, CASP1* and *IRF2* using the TIMER database. As shown in Fig. 8A–D, the expression of *PAFAH1B3* was significantly negatively correlated with *NLRP3, NLRP1, CASP1* and *IRF2* in LUAD. We further used the GEPIA database to verify these associations and found that *PAFAH1B3* was significantly negatively correlated with *NLRP3, NLRP1, CASP1* and *IRF2* in LUAD (Fig. 8E–H). Subsequently, we used TCGA database to further analyze the differential expression of *NLRP1, NLRP3, NLRP1* and *CASP1* and *IRF2* in lung adenocarcinoma tissues and normal lung tissues, and simultaneously explored the survival curves of these pyroptotic genes, and finally found that *NLRP 3, NLRP 1, CASP1* and *IRF2* were significantly low expression in lung adenocarcinoma tissues and *NLRP3* (Fig. 9A-D) and low expression of *NLRP1, NLRP3* predicted poor patient prognosis (Fig. 9E-H). Relevant studies have found that

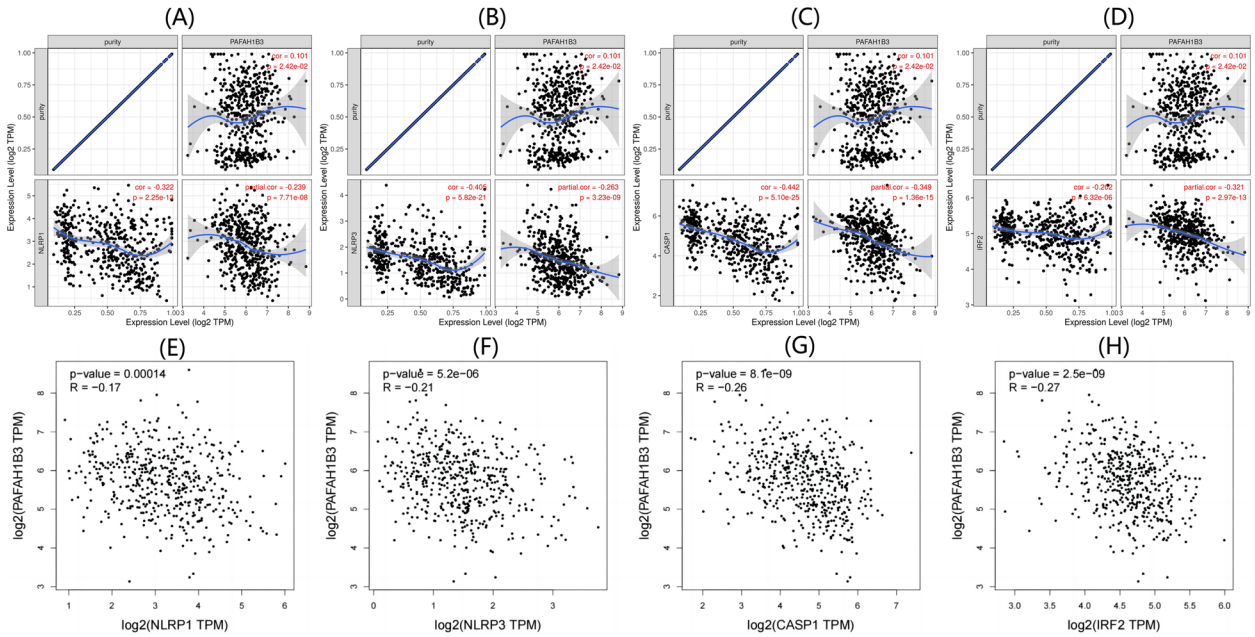

Fig. 8 Correlation of *PAFAH1B3* expression with *NLRP3, NLRP1, CASP1* and *IRF2* expression in LUAD. **A**–**D** Spearman correlation analysis of *PAFAH1B3* with *NLRP3, NLRP1, CASP1* and *IRF2* expression in LUAD. **E**–**H** Correlation of *PAFAH1B3* expression with *NLRP3, NLRP1, CASP1* and *IRF2* in LUAD as determined by GEPIA database

NLRP1, NLRP3, IRF2, and *CASP1* are widely involved in the pyroptosis and immune infiltration of various tumors [11]. And *CASP1* can inhibit the growth and invasion of non-small-cell lung cancer (NSCLC) [12]. These results suggest that the high expression of *PAFAH1B3* inhibits the pyroptosis of LUAD cells, leading to tumor progression and poor prognosis.

Discussion

In this study, we first analyzed *PAFAH1B3* expression in pan-cancer using TCGA database and then used the GEPIA database to validate the expression of *PAFAH1B3* observed in TCGA pan-cancer data. We further found that LUAD patients with high *PAFAH1B3* expression had a poor prognosis. A previous study found *PAFAH1B3* was an independent prognostic risk factor for LUAD [13]. This is consistent with the results of our study.

To explore the upstream regulatory miRNAs of *PAFAH1B3*, we used the starBase database to predict miRNAs that might bind to *PAFAH1B3*. In total, 14 candidate miRNAs were identified. Some of these miRNAs have been shown to function as tumor suppressor miRNAs in LUAD. For example, *hsa-miR-24-3p* was shown to decrease AVL9 expression, which inhibited tumor development in non-small cell lung cancer [14]. *hsa-miR-101-3p* inhibits LUAD cell growth by reducing CEP55 expression [15]. Survival of LUAD patients was highly related with *hsa-miR-29c-3p* [16]. Through correlation, expression, and survival analyses in this study, *hsa-miR-29c-3p* was identified as a potential upstream miRNA that suppresses *PAFAH1B3*.

Furthermore, the putative lncRNAs of the *hsa-miR-29c-3p*/*PAFAH1B3* axis should be carcinogenic lncRNAs, according to the ceRNA hypothesis [17]. Consequently, we explored the lncRNAs upstream of the *hsa-miR-29c-3p*/*PAFAH1B3* axis and identified 30 potential lncRNAs. Expression analysis, survival analysis, and correlation analysis identified *DUXAP8* as an lncRNA that potentially regulates the *hsa-miR-29c-3p*/*PAFAH1B3* axis. *DUXAP8* has been shown to promote cancer by activating the Akt/mTOR signaling pathway [18]. *DUXAP8* also influences the activity of miRNAs [19]. High *DUXAP8* expression in NSCLC was shown to be related with poor patient prognosis, and *DUXAP8* plays a role in NSCLC cell proliferation, epithelial-mesenchymal transition, and aerobic glycolysis [20]. In addition, it has also been found that *DUXAP8* promotes the proliferation and migration of ovarian cancer cells by down-regulating the expression of microRNA-29. It has also been found that the DUXAP8-miR-29-3p axis can influence hepatocellular carcinoma immune infiltration [21]. This laterally validated our predicted *DUXAP8-microRNA-29c-3p-PAFAH1B3* pathway [22].

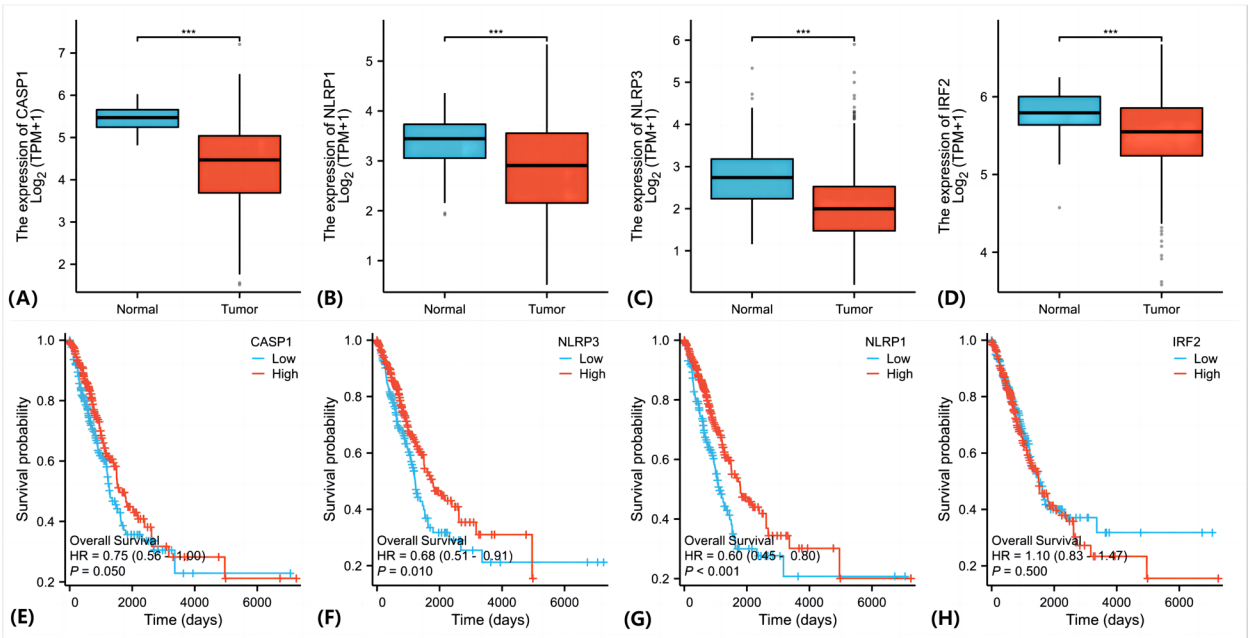

Fig. 9 Expression and prognosis analysis of *NLRP 3, NLRP 1*, and *CASP1* and *IRF2* in LUAD. **A**–**D** The Wilcoxon rank sum test was used to compare the differences between *NLRP 3, NLRP 1, CASP1* and *IRF2* in LUAD and normal lung tissue in TCGA database, and *NLRP 3, NLRP 1, CASP1* and *IRF2* were all low expressed in LUAD. **E**–**H** The expression of the target genes in LUAD patients is ranked in the TCGA database, with the first 50 percent set as low expression and the last 50 percent as high expression. The OS of *NLRP 3*, and *NLRP 1* high and low expression groups were significantly different

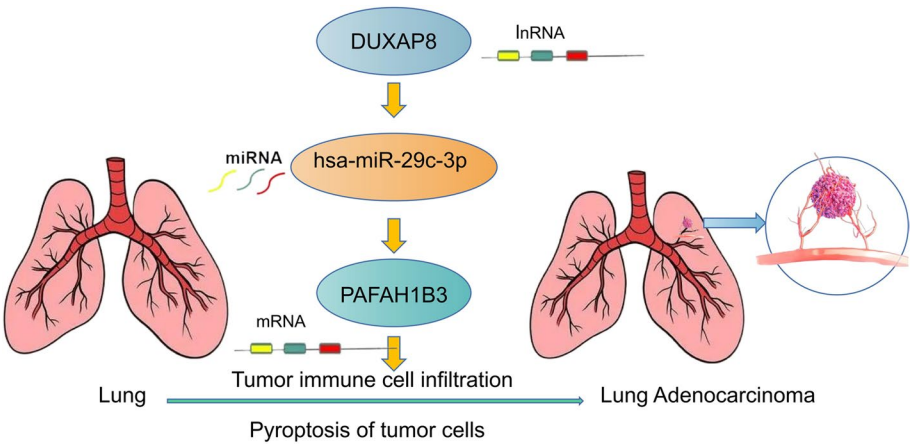

Fig. 10 The *DUXAP8-hsa-miR-29c-3p-PAFAH1B3* axis in lung adenocarcinoma

In this study, *PAFAH1B3* was found to be strongly adversely linked with numerous immune cells in LUAD. Furthermore, *PAFAH1B3* was strongly inversely associated with biomarkers of these invading immune cells. The degree of tumor immune cell infiltration is closely connected to the prognosis of NSCLC [23]. These data suggest that aberrant *PAFAH1B3* overexpression leads to abnormal LUAD immune cell infiltration and poor expression of biomarkers of immune cells.

Pyroptosis, a new form of non-apoptotic programmed cell death that is mediated by an inflammatory response, is associated with many diseases [24]. Pyroptosis was found to eliminate anti-apoptotic or anti-necrotic cancer cells in lung cancer [25]. Our results showed that high expression of *PAFAH1B3* in LUAD correlated with reduced expression of NLRP3, NLRP1, Casp1 and IRF2, which are related to pyroptosis [26]. This further suggests that high expression of *PAFAH1B3* will affect patient prognosis.

In conclusion, we discovered that *PAFAH1B3* is highly expressed in a variety of human malignancies, including LUAD, and that its high expression in LUAD correlates with poor prognosis. Our results suggest that the *DUXAP8-hsa-miR-29c-3p* axis may regulate *PAFAH1B3* in LUAD (Fig. 10). Furthermore, we discovered that *PAFAH1B3* exerts tumor promoting functions by reducing tumor immune cell infiltration and the expression of related localized death genes. These findings should be verified by additional research and clinical trials.

Acknowledgements
This study was supported by the National Postdoctoral Innovation Talents Support Program of China, and National Natural Science Foundation of China (No. 82303564).

Authors' contributions
Bowen Hu: Data curation (lead); formal analysis (lead); methodology (equal). Lingyu Du: Investigation (equal); methodology (equal). Guangda Yuan: Data curation (equal); formal analysis (equal); funding acquisition (equal). Yong Yang: Formal analysis (equal); resources (equal). Ming Li: Conceptualization (equal); writing – original draft (equal). Jie Tan: Conceptualization (equal); writing – original draft, review and editing (equal). All authors have contributed sufficiently to the work to accept responsibility for the study and have agreed to be held accountable for all aspects of the work.

Availability of data and materials
The molecular experiment data generated and analyzed during the current study are available from the corresponding author on reasonable request.
1. Data from public databases
(1) All experimental data supporting this study are publicly available and have been stored in TCGA database (https://portal.gdc.cancer.gov/), GEPIA database (http://gepia.cancer-pku.cn/), Starbase database (http://starbase.sysu.edu.cn/) and TIMER database (https://cistrome.shinyapps.io/timer/).
(2) Some of the public data processed are presented in the supplementary material.
2. Data results from experiments
All experimental results are presented in figures in the manuscript.

Declarations

Ethics approval and consent to participate
The study was approved by the Ethics Committee of Nanjing Medical University (approval number: K-2020–043-H01). All patients provided written informed consent through a process that was reviewed by the Ethics Committee of Nanjing Medical University. This study was performed in accordance with the ethical standards laid out in the Helsinki Declaration of 1964.

Competing interests
The authors declare that the research was conducted in the absence of any commercial or financial relationships that could be construed as a potential conflict of interest.

Author details
[1]Department of Thoracic Surgery, The Affiliated Suzhou Hospital of Nanjing Medical University, Suzhou, Jiangsu, China. [2]Department of Oncology, The Affiliated Suzhou Hospital of Nanjing Medical University, Suzhou, Jiangsu, China. [3]Department of Thoracic Surgery, Zhongshan Hospital Affiliated to Fudan University, Shanghai, China.

Received: 17 October 2023 Revised: 10 January 2024 Accepted: 16 January 2024
Published online: 04 February 2024

References

1. Cancer.World Health Organization https://www.who.int/news-room/fact sheets/detail/cancer; 2018.
2. Bray F, Ferlay J, Soerjomataram I, Siegel RL, Torre LA, Jemal A. Global cancer statistics 2018: GLOBOCAN estimates of incidence and

mortality worldwide for 36 cancers in 185 countries. CA Cancer J Clin. 2018;68(6):394–424.
3. Xie T, Guo X, Wu D, Li S, Lu Y, Wang X, Chen L. PAFAH1B3 expression is correlated with gastric cancer cell proliferation and immune infiltration. Front Oncol. 2021;11:591545. https://doi.org/10.3389/fonc.2021.591545.PMID:33732641;PMCID:PMC7959814.
4. Jiang W, Quan R, Bhandari A, Hirachan S, Chen C, Lv S, Zheng C. PAFAH1B3 regulates papillary thyroid carcinoma cell proliferation and metastasis by affecting the EMT. Curr Med Chem. 2024;31(9):1152–64. https://doi.org/10.2174/0929867330666230427102920. PMID: 37102492.
5. Yuan Y, Jiang X, Tang L, Wang J, Duan L. Comprehensive analysis of the prognostic and immunological role of PAFAH1B in pan-cancer. Front Mol Biosci. 2022;8: 799497.
6. Gao S, Ding B, Lou W. microRNA-Dependent modulation of genes contributes to ESR1's effect on ERα positive breast cancer. Front Oncol. 2020;10:753.
7. Ghafouri-Fard S, Shoorei H, Anamag FT, Taheri M. The role of non-coding RNAs in controlling cell cycle related proteins in cancer cells. Front Oncol. 2020;10:608975.
8. Tang Z, Li C, Kang B, Gao G, Li C, Zhang Z. GEPIA: a web server for cancer and normal gene expression profiling and interactive analyses. Nucleic Acids Res. 2017;45(W1):W98–102.
9. Li JH, Liu S, Zhou H, Qu LH, Yang JH. starBase v2.0: decoding miRNA-ceRNA, miRNA-ncRNA and protein-RNA interaction networks from large-scale CLIP-Seq data. Nucleic Acids Res. 2014;42:D92–7.
10. Li T, Fan J, Wang B, Traugh N, Chen Q, Liu JS, Li B, Liu XS. TIMER: a web server for comprehensive analysis of tumor-infiltrating immune cells. Cancer Res. 2017;77:e108–10.
11. Karki R, Man SM, Kanneganti TD. Inflammasomes and Cancer. Cancer Immunol Res. 2017;5(2):94–9. https://doi.org/10.1158/2326-6066.CIR-16-0269. Epub 2017. PMID: 28093447; PMCID: PMC5593081.
12. Huang T, Zhang P, Li W, Zhao T, Zhang Z, Chen S, Yang Y, Feng Y, Li F, Shirley Liu X, Zhang L, Jiang G, Zhang F. G9A promotes tumor cell growth and invasion by silencing CASP1 in non-small-cell lung cancer cells. Cell Death Dis. 2017;8(4):e2726. https://doi.org/10.1038/cddis.2017.65.PMID:28383547;PMCID:PMC5477595.
13. Tang S, Ni J, Chen B, Sun F, Huang J, Ni S, Tang Z. PAFAH1B3 predicts poor prognosis and promotes progression in lung adenocarcinoma. BMC Cancer. 2022;22(1):525.
14. Wei D, Sun L, Feng W. hsa_circ_0058357 acts as a ceRNA to promote non-small cell lung cancer progression via the hsa-miR-24-3p/AVL9 axis. Mol Med Rep. 2021;23(6):470.
15. Ji L, Yang T, Liu M, Li J, Si Q, Wang Y, Liu J, Dai L. Construction of lncRNA TYMSOS/hsa-miR-101-3p/CEP55 and TYMSOS/hsa-miR-195-5p/CHEK1 Axis in Non-small Cell Lung Cancer. Biochem Genet. 2023;61(3):995–1014. https://doi.org/10.1007/s10528-022-10299-0.
16. Yu DH, Ruan XL, Huang JY, Liu XP, Ma HL, Chen C, Hu WD, Li S. Analysis of the interaction network of hub miRNAs-hub genes, being involved in idiopathic pulmonary fibers and its emerging role in non-small cell lung cancer. Front Genet. 2020;11:302.
17. Salmena L, Poliseno L, Tay Y, Kats L, Pandolfi PP. A ceRNA hypothesis: the Rosetta Stone of a hidden RNA language? Cell. 2011;146(3):353–8.
18. Lei C, Li S, Fan Y, Hua L, Pan Q, Li Y, Long Z, Yang R. LncRNA DUXAP8 induces breast cancer radioresistance by modulating the PI3K/AKT/mTOR pathway and the EZH2-E-cadherin/RHOB pathway. Cancer Biol Ther. 2022;23(1):1–13. https://doi.org/10.1080/15384047.2022.2132008.PMID:36329030;PMCID:PMC9635553.
19. Wang B, Xu W, Cai Y, Chen J, Guo C, Zhou G, Yuan C. DUXAP8: a promising lncRNA with carcinogenic potential in cancer. Curr Med Chem. 2022;29(10):1677–86.
20. Wu C, Song W, Wang Z, Wang B. Functions of lncRNA DUXAP8 in non-small cell lung cancer. Mol Biol Rep. 2022;49(3):2531–42.
21. Zhang L, Hu S, Chen J, Ma S, Liu F, Liu C, Gao Y. Comprehensive analysis of the MIR4435-2HG/miR-1-3p/MMP9/miR-29-3p/DUXAP8 ceRNA network axis in hepatocellular carcinoma. Discov Oncol. 2021;12(1):38. https://doi.org/10.1007/s12672-021-00436-3.PMID:35201491;PMCID:PMC8777520.
22. Li LM, Hao SJ, Ni M, Jin S, Tian YQ. DUXAP8 promotes the proliferation and migration of ovarian cancer cells via down-regulating microRNA-29a-3p expression. Eur Rev Med Pharmacol Sci. 2021;25(4):1837–44. https://doi.org/10.26355/eurrev_202102_25078. PMID: 33660793.
23. Sun H, Sui B, Li Y, Yan J, Cao M, Zhang L, Liu S. Analysis of the significance of immune cell infiltration and prognosis of non-small-cell lung cancer by bioinformatics. J Healthc Eng. 2021;2021:3284186.
24. Broz P, Pelegrín P, Shao F. The gasdermins, a protein family executing cell death and inflammation. Nat Rev Immunol. 2020;20(3):143–57.
25. Chen X, Wu J, Wang J. Pyroptosis: a new insight of non-small-cell lung cancer treatment. Front Oncol. 2022;12:1013544.
26. Teng JF, Mei QB, Zhou XG, Tang Y, Xiong R, Qiu WQ, Pan R, Law BY, Wong VK, Yu CL, Long HA, Xiao XL, Zhang F, Wu JM, Qin DL, Wu AG. Polyphyllin VI induces caspase-1-mediated pyroptosis via the induction of ROS/NF-κB/NLRP3/GSDMD signal axis in non-small cell lung cancer. Cancers (Basel). 2020;12(1):193.

Publisher's Note